

Ocular Factors of Fractal Dimension and Blood Vessel Tortuosity Derived From OCTA in a Healthy Chinese Population

Yunhe Song^{1,*}, Weijing Cheng^{1,*}, Fei Li¹, Fengbin Lin¹, Peiyuan Wang¹, Xinbo Gao¹, Yuying Peng¹, Yuhong Liu¹, Hengli Zhang², Shiyan Chen³, Yazhi Fan⁴, Ran Zhang⁵, Wei Wang¹, and Xiulan Zhang¹

¹ State Key Laboratory of Ophthalmology, Zhongshan Ophthalmic Center, Sun Yat-sen University, Guangdong Provincial Key Laboratory of Ophthalmology and Visual Science, Guangdong Provincial Clinical Research Center for Ocular Diseases, Guangzhou, China

² Department of Ophthalmology, Shijiazhuang People's Hospital, Shijiazhuang, China

³ Department of Ophthalmology, Sichuan Academy of Medical Sciences & Sichuan Provincial People's Hospital, Chengdu, China

⁴ The Second Affiliated Hospital of Xi'an Jiaotong University, Shaanxi, China

⁵ Mianyang Central Hospital, School of Medicine, University of Electronic Science and Technology of China, Mianyang, China

Correspondence: Xiulan Zhang, State Key Laboratory of Ophthalmology, Zhongshan Ophthalmic Center, Sun Yat-sen University, Guangdong Provincial Key Laboratory of Ophthalmology and Visual Science, Guangdong Provincial Clinical Research Center for Ocular Diseases, Guangzhou 510060, China.

e-mail: zhangxl2@mail.sysu.edu.cn

Wei Wang, State Key Laboratory of Ophthalmology, Zhongshan Ophthalmic Center, Sun Yat-sen University, Guangdong Provincial Key Laboratory of Ophthalmology and Visual Science, Guangdong Provincial Clinical Research Center for Ocular Diseases, Guangzhou 510060, China.

e-mail: zoc_wangwei@yahoo.com

Received: December 1, 2021

Accepted: April 6, 2022

Published: May 2, 2022

Keywords: glaucoma; fractal dimension; blood vessel tortuosity; OCTA; Chinese

Citation: Song Y, Cheng W, Li F, Lin F, Wang P, Gao X, Peng Y, Liu Y, Zhang H, Chen S, Fan Y, Zhang R, Wang W, Zhang X. Ocular factors of fractal dimension and blood vessel tortuosity derived from OCTA in a healthy Chinese population. *Transl Vis Sci Technol.* 2022;11(5):1, <https://doi.org/10.1167/tvst.11.5.1>

Purpose: To identify the ocular factors of microvascular fractal dimension (FD) and blood vessel tortuosity (BVT) of macula measured with optical coherence tomography angiography (OCTA) in a healthy Chinese population.

Methods: Healthy subjects without ocular disorders were recruited at Zhongshan Ophthalmic Center. The FD and BVT in the superficial capillary plexus (SCP) and deep capillary plexus (DCP) at the macula were obtained from OCTA images. The FD was calculated using the box-counting method, and the BVT was defined as the ratio of the actual distance between two points to the straight distance on the skeletonized image. Univariate and stepwise multivariate linear regression analyses were performed to identify the ocular factors of FD and BVT, and the results are presented as coefficients and 95% confidence intervals (CIs). Only the right eye of each subject was included.

Results: A total of 2189 healthy individuals (2189 eyes) were included with a mean age of 49.9 ± 13.2 years; 54.4% were female. In the multivariate model, the FD in the SCP was significantly associated with higher intraocular pressure (IOP) ($\beta = 0.204$; 95% CI, 0.073–0.335; $P < 0.001$), axial length (AL) ($\beta = -0.875$; 95% CI, -1.197 to -0.552 ; $P < 0.001$; $R^2 = 0.26$; root mean square error [RMSE] = 7.78). The FD in the DCP was significantly associated with best-corrected visual acuity ($\beta = -6.170$; 95% CI, -10.175 to -2.166 ; $P = 0.003$) and anterior chamber depth ($\beta = -0.348$; 95% CI, -0.673 to -0.023 ; $P = 0.036$; $R^2 = 0.10$; RMSE = 2.58). Superficial BVT was independently associated with IOP ($\beta = -0.044$; 95% CI, -0.079 to -0.009 ; $P = 0.012$) and AL ($\beta = 0.097$; 95% CI, 0.014–0.181; $P = 0.022$; $R^2 = 0.15$; RMSE = 2.02). Deep BVT was independently associated with IOP ($\beta = -0.004$; 95% CI, -0.009 to -0.0005 ; $P = 0.028$) and lens thickness ($\beta = 0.036$, 95% CI, 0.003–0.060; $P = 0.028$; $R^2 = 0.07$, RMSE = 0.25).

Conclusions: The IOP and AL were dependent ocular parameters variables of FD and BVT in the SCP in this healthy population. The FD in the DCP was also influenced by visual acuity and anterior chamber depth. These factors should be considered when microvascular geometrics are used in the future studies.

Translational Relevance: This work discovered the influence factors of OCTA geometrics parameters for further establishment of diagnostic model or method for glaucoma and other microvasculature-related ocular diseases.

Introduction

Glaucoma remains the leading cause of irreversible blindness worldwide.^{1,2} An insufficiency of blood perfusion has been identified as a potential pathogenic factor of glaucoma.^{3,4} The literature has documented close associations between decreased vessel density and glaucoma severity.^{3,5-8} Apart from flow metrics, the vessel geometric parameters were also recently recognized as biomarkers for glaucoma.⁹

Retinal vascular fractal dimension (FD) and blood vessel tortuosity (BVT) have been the most used geometric parameters, as they quantitatively reflect the complexity of retinal vasculature branching.^{10,11} Few studies have shown a correlation between blood vessel complexity and glaucoma, and their results have been inconsistent. Rudnicka et al.¹² reported that less tortuous retinal arterioles and venules were associated with all subtypes of glaucoma, but only significantly for glaucoma suspect. Lin and colleagues¹¹ found that normal tension glaucoma was associated with decreased arteriolar and venular tortuosity. This discrepancy may arise from the limitations of fundus photography, which shows only the complexity of large vessels and not the microvasculature. In addition, traditional photography cannot evaluate the retinal vasculature in different layers.

The emergence and evolution of optical coherence tomography angiography (OCTA) have enabled the visualization and quantification of retinal microvasculature in vivo and non-invasively.¹³ Using OCTA, the FD and BVT were found to be lower in normal-tension glaucoma with systemic hypertension compared to normal controls, whereas macular vessel branching complexity was not related to the severity of visual field loss.¹⁴ This finding still applies to the patients with ocular hypertension and glaucoma suspect.⁹ However, whether the FD and BVT are associated with glaucoma in different retinal layers is still under debate. Before initiating wide application of these parameters, their distribution and other factors should be systematically evaluated in a healthy population, but we are unaware of this type of study in a relatively large sample population.

To fill this knowledge gap, the present study aimed to investigate the ocular factors of FD and BVT in a large sample of a healthy Chinese population using swept-source OCTA (SS-OCTA) to provide improved interpretation of microvasculature and associated factors that would be useful for further studies on glaucoma and other ocular diseases.

Methods

Study Population

This cross-sectional study was conducted at the Zhongshan Ophthalmic Center (ZOC), Sun Yat-sen University, Guangzhou, China. The study protocol was approved by the ethical committee of ZOC (2018KYPJ126) and was conducted in accordance with the tenets of the Declaration of Helsinki. Written informed consent was obtained from all subjects.

Healthy subjects >30 years of age were enrolled in this study. Subjects were excluded if they met any of the following criteria: (1) best-corrected visual acuity (BCVA) less than 20/40 in the study eye; (2) intraocular pressure (IOP) >21 mm Hg; (3) spherical equivalent > +6.0 diopters (D) or < -6.0 D; (4) axial length (AL) \geq 26 mm; (5) any previous or current ocular disorders or surgeries (i.e., corneal disorders, cataract, uveitis, ocular trauma, glaucoma, diabetic retinopathy, and retinal detachment); (6) a history of systemic cardiovascular or neurodegenerative diseases (e.g., hypertension, diabetes, hyperlipidemia, ischemic stroke, Alzheimer's disease); and (7) glaucomatous or retinal disorder evidenced by fundus photography or OCT, cup-to-disc ratio asymmetry > 0.2, retinal nerve fiber layer defect, or epiretinal membrane.

Collection of Systemic and Ocular Factors

Subjects were interviewed by clinical research collaborators who used a standardized questionnaire to collect the subjects' demographics and history of ocular and systemic diseases. Blood pressure was measured twice at a quiet state using an automated blood pressure monitor (HEM-1000; Omron Corporation, Kyoto, Japan), and the average systolic blood pressure (SBP) and diastolic blood pressure (DBP) measurements were recorded. Weight and height were measured using automated meters.

Comprehensive ophthalmic examinations were performed in all subjects and included anterior and posterior segment examination using slit-lamp biomicroscopy (BQ-900; Haag-Streit, Köniz, Switzerland) and an indirect ophthalmoscope (MaxLight Standard 90D Slit Lamp Lenses; Ocular Instruments, Bellevue, WA). IOP measurement was conducted using a Goldmann applanation tonometer (AT900; Haag-Streit), and the means of three consecutive measurements were recorded; visual acuity and BCVA measurement was conducted using Early Treatment Diabetic

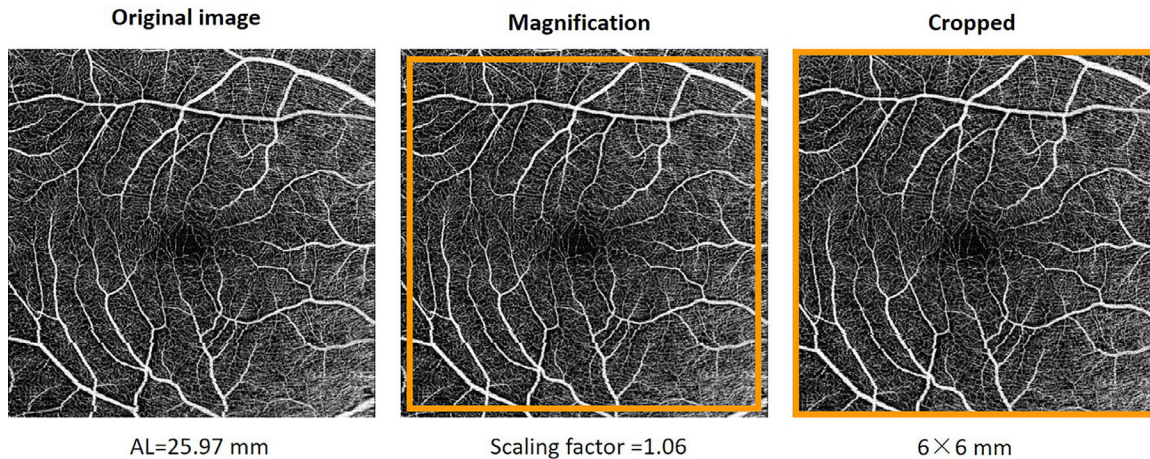


Figure 1. Magnification correction by using Littmann's method and the Bennett formula. Scaling factor = $3.382 \times 0.013062 \times (AL - 1.82)$. The scaling factor represents the magnification effect, and AL represent the axial length. The scaling factor equals to 1 if AL equals 23.82 mm. An en face image of the SCP at the macula with AL = 24.81 mm is presented, and the scaling factor was calculated as 1.02. The orange square represents the actual image size that corresponds to 6×6 mm. The cropped images were involved in the final analysis.

Retinopathy Study (ETDRS) visual acuity charts (Precision Vision, Villa Park, IL) at a distance of 4 meters. Ocular biometry measurement was conducted using the IOLMaster 700 (Carl Zeiss Meditec, Dublin, CA) and included AL, central corneal thickness, lens thickness (LT), and anterior chamber depth (ACD).

SS-OCT and SS-OCTA Imaging and Quantification

SS-OCT and SS-OCTA images were captured in a dark room after pupil dilatation by experienced technicians. High-resolution structural and microvascular images were acquired using SS-OCT (DRI OCT Triton; Topcon Healthcare, Tokyo, Japan). The instrument was equipped with a wavelength of 1050 nm and performed 100,000 A-scans per second with axial and lateral resolutions of $8 \mu\text{m}$ and $20 \mu\text{m}$, respectively. The scanning protocol was conducted as 6×6 mm centered on the central fovea and 7×7 mm of the optic nerve head with 320×320 A-scans. The peripapillary retinal nerve fiber layer (pRNFL) and ganglion cell–inner plexiform layer (GCIPL) were segmented and automatically measured using pre-installed software. For the OCTA image, motion artifacts and projection artifacts were eliminated using the built-in software with active eye tracker and projection artifact removal. Automatic image segmentation was performed using IMAGENet 6 (version 1.23; Topcon Healthcare). Image quality scores (IQSs), with a range of 0 to 100, were automatically obtained from each

scan using built-in software. Any image with an IQS below 40 was excluded. Additionally, two graders performed an independent qualification control of OCTA image artifacts, and those with typical artifacts were excluded. The artifacts were divided into five categories based on previous studies: motion, defocus, decentration, segmentation errors, and masking.^{15,16}

Following projection artifact removal using the function in IMAGENet software, the images were adjusted for magnification effects using Littmann's method and the Bennett formula (Fig. 1).^{17,18} The images were automatically binarized using Huang's method and skeletonized accordingly using ImageJ software (National Institutes of Health, Bethesda, MD).¹⁹ The FD was calculated by the box-counting method,^{20,21} in which a count is comprised of the number of squares subtended by pattern in each skeletonized OCTA scan, and the count is repeated as the size of the squares of the grid declines. The box size was defined as 2 pixels, and the maximum size was 45% of the total image scale (6×6 mm, 1024×1024 pixels).

The calculated slope of the fitting regression line was defined as the FD value (Fig. 2), and the plot was fitted with the least squares method. BVT was calculated as the ratio (sum of branch lengths divided by the sum of imaginary straight lines) of the actual distance between two points to the straight distance based on the skeletonized image (Fig. 3).²² The box-counting and BVT calculations were carried out using Image J software. Unqualified OCTA images were excluded from the analysis.

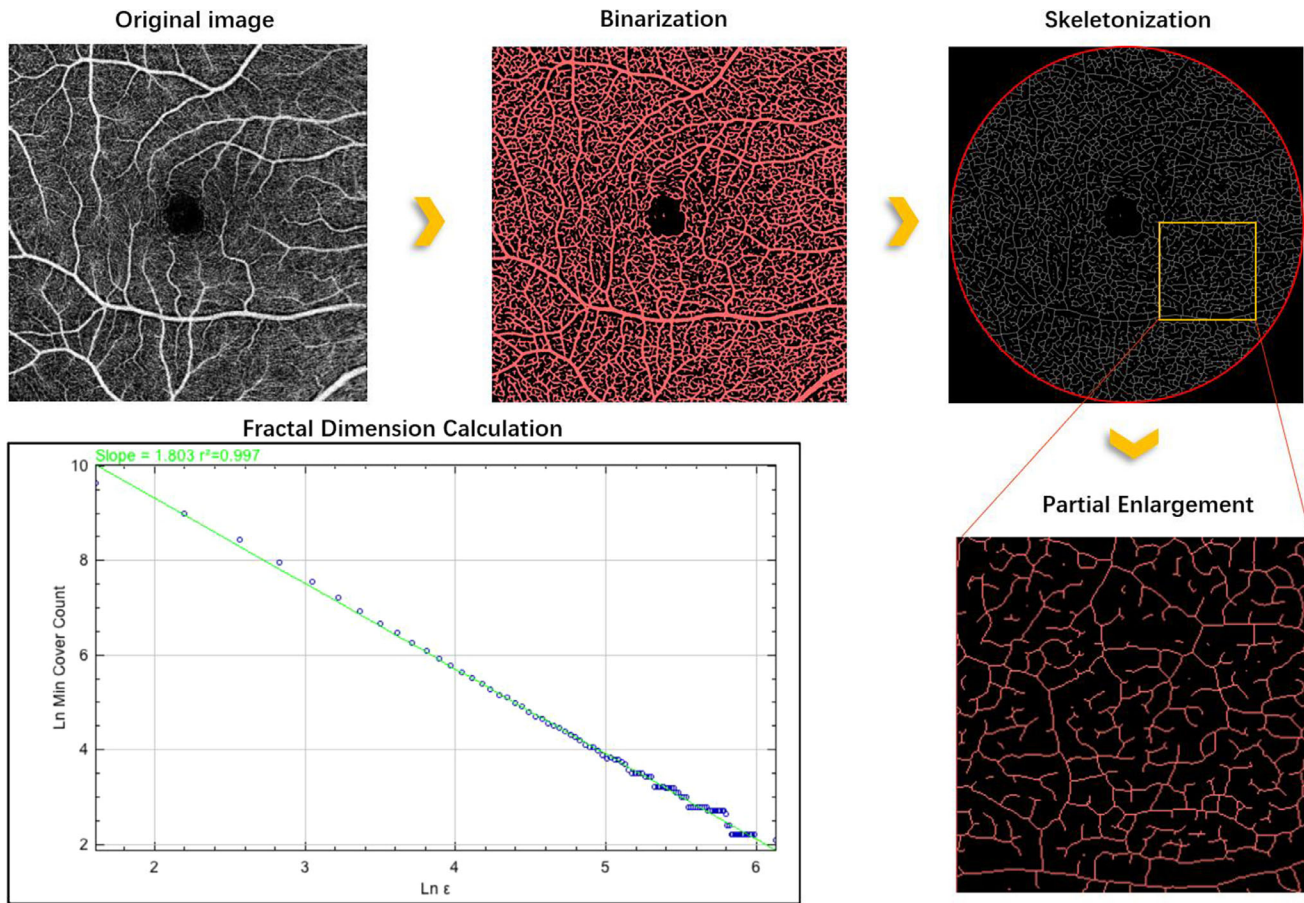


Figure 2. Schematic illustration of the retinal microvascular FD measurement and parameter extraction from a subject who was 43 years old. Images of the macula were obtained by OCTA B-scans. The 6×6 -mm scans of en face blood flow images of both superficial and deep retina were stratified. Original images with a scan size of 6×6 mm were obtained following the removal of projection artifacts. Binarized and skeletonized capillary images were then obtained. The *blue dot* represents actual OCTA data for this image, and the *green line* displays the closest fitting fractal log–log line. The x-axis indicates the log base e of the size of the boxes in pixels, and the y-axis represents the log base e of the number of boxes subtending the OCTA pattern. Thus, a linear relationship in the log–log plot is an indication of perfect self-similarity, and the high correlation demonstrates a high degree of self-similarity in OCTA patterns.

Statistical Analysis

Data from the right eye of each subject were used for statistical analysis. The descriptive statistics are presented as means, standard deviations, and frequencies of the variables of demographic, ocular biometry, and OCTA data variables. Univariate and stepwise multivariate regression models were used to determine the relationship between FD and BVT (dependent variables) and ocular factors (independent variables). Factors that were found to be significant in the univariate analysis ($P < 0.10$) were included in multivariate regression. All P values were two sided and considered statistically significant at $P < 0.05$. Statistical analysis was performed using Stata/MP 16.0 (StataCorp LLC, College Station, TX).

Results

Characteristics of Subjects

A total of 2801 eyes from 2801 subjects were initially recruited for this study. A total of 612 subjects (612 eyes) were excluded from the study for the following reasons: BCVA below 20/20 ($n = 5$), IOP > 21 mm Hg ($n = 12$), high myopia or high hyperopia ($n = 21$), RNFL defect ($n = 3$), history of previous systemic cardiovascular or neurodegenerative disease ($n = 12$), ocular and systemic medications ($n = 2$), and alcohol, coffee, and heavy water consumption ($n = 3$). Those with poor IQSs were also excluded ($n = 554$). Finally, the remaining 2189 subjects (2189 eyes) were analyzed. [Table 1](#) shows the demographic and clinical

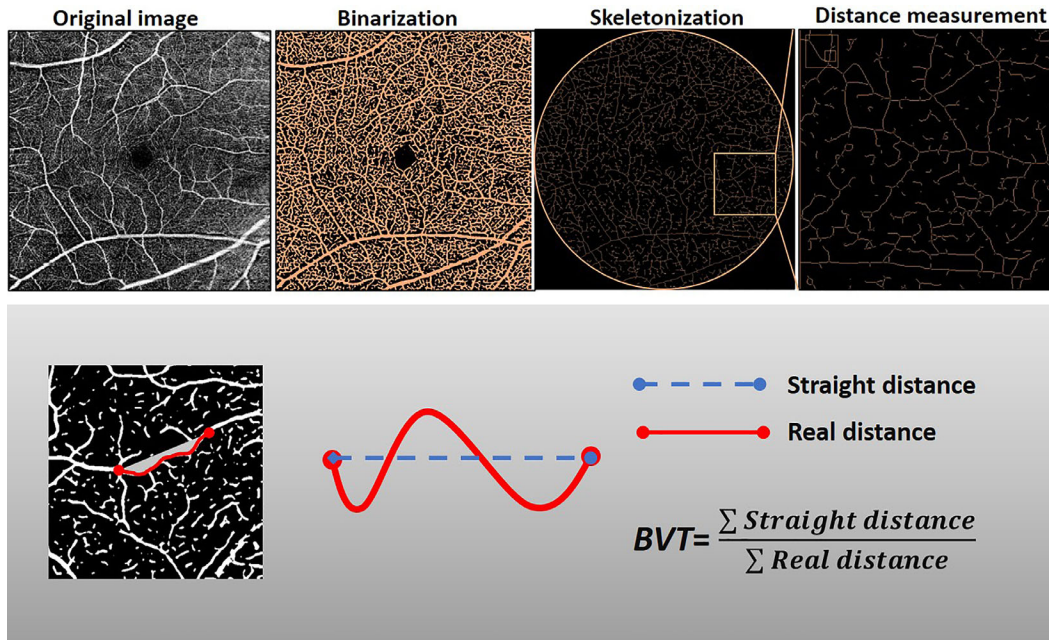


Figure 3. Schematic illustration of the retinal microvascular BVT measurement and parameter extraction. Images of the macula were obtained by OCTA B-scans. The 6 × 6-mm scans of en face blood flow images of both superficial and deep retina were stratified. Original images with a scan size of 6 × 6 mm were obtained following the removal of projection artifacts. Binarized and skeletonized capillary images were then generated to extract the distance parameters for BVT calculation. The BVT was calculated as the sum of real distances of the vessel branch divided by the sum of straight distances.

Table 1. Clinical Characteristics of the Study Population

Characteristic	
Number of subjects (eyes), <i>n</i>	2801 (2801)
Female, <i>n</i> (%)	1900 (67.83)
Age (yr), mean ± SD	54.1 ± 14.5
SBP (mm Hg), mean ± SD	126.13 ± 19.32
DBP (mm Hg), mean ± SD	69.21 ± 10.63
Height (cm), mean ± SD	159.59 ± 7.74
Weight (kg), mean ± SD	59.71 ± 10.8
Body mass index (kg/m ²), mean ± SD	23.39 ± 3.48
BCVA (logMAR), mean ± SD	0.14 ± 0.21
IOP (mm Hg), mean ± SD	15.36 ± 2.64
ACD (mm), mean ± SD	2.78 ± 0.56
Lens thickness (mm), mean ± SD	4.42 ± 0.47
AL (mm), mean ± SD	23.77 ± 1.17
Average GCIPL thickness (μm), mean ± SD	70.58 ± 6.16
Average pRNFL thickness (μm), mean ± SD	109.47 ± 14.04
Image quality index, mean ± SD	69.46 ± 9.17

characteristics of the participants. The mean age was 49.9 years, and 54.4% were female.

Distribution of FD and BVT

For calculation purposes, the values of FD and BVT were expanded by a factor of 1000. The FD and BVT were 1790.95 ± 9.04 and 1007.46 ± 2.18, respectively, in the superficial capillary plexus (SCP). The average FD and BVT were 1865.56 ± 3.19 and 1004.55 ± 0.25, respectively, in the deep capillary plexus (DCP). The reference values are listed in Table 2.

Ocular Factors of FD in Each Layer

Table 3 shows the univariate and multivariate regression analyses of superficial and deep FDs. After adjusting for age, sex, and IQS, the superficial FD was significantly correlated with IOP ($\beta = 0.204$; 95% confidence interval [CI], 0.073–0.335; $P < 0.001$) and AL ($\beta = -0.875$; 95% CI, -1.197 to -0.552; $P < 0.001$; $R^2 = 0.26$; RMSE = 7.79). In the DCP, after adjusting for the confounding factors, the BCVA ($\beta = -6.170$; 95% CI, -10.105 to -2.166; $P < 0.001$) and anterior chamber depth ($\beta = -0.348$; 95% CI, -1.197 to -0.552; $P < 0.001$) were associated with FD ($R^2 = 0.10$; RMSE = 2.58).

Table 2. Distribution of Retinal Microvasculature Geometric Parameters Values

	Centile							Mean \pm SD
	5th	10th	25th	50th	75th	90th	95th	
FD in SCP ($\times 10^{-3}$)	1773.0	1778.2	1786.0	1793.0	1797.6	1800.5	1802.3	1790.3 \pm 9.1
FD in DCP ($\times 10^{-3}$)	1859.6	1862.2	1864.6	1866.3	1867.5	1868.3	1868.7	1864.9 \pm 3.2
BVT in SCP ($\times 10^{-3}$)	1005.1	1005.3	1005.8	1006.9	1008.5	1010.4	1011.8	1007.5 \pm 2.2
BVT in DCP ($\times 10^{-3}$)	1004.3	1004.3	1004.4	1004.5	1004.7	1004.8	1005.0	1004.6 \pm 0.3

Table 3. Univariate and Multivariate Regression Analyses for Superficial and Deep Fractal Dimensions

Characteristics	Univariate Regression		Stepwise Multivariate Regression	
	Coefficient (95% CI)	<i>P</i>	Coefficient (95% CI)	<i>P</i>
Superficial capillary plexus				
Female sex	−0.776 (−1.600, −0.048)	0.065	—	—
Mean age (yr)	0.019 (−0.009, 0.047)	0.199	—	—
BCVA (logMAR)	−11.292 (−23.247, 0.663)	0.064	—	—
IOP (mm Hg)	0.305 (0.155, 0.456)	<0.001	0.204 (0.073, 0.335)	<0.001
ACD (mm)	−2.203 (−2.914, −1.493)	<0.001	—	—
Lens thickness (mm)	0.887 (0.027, 1.74)	<0.001	—	—
AL (mm)	−1.754 (−2.073, −1.436)	<0.001	−0.875 (−1.197, −0.552)	<0.001
GCIPL thickness (μ m)	0.079 (−0.005, 0.163)	0.067	—	—
pRNFL thickness (μ m)	0.054 (0.018, 0.091)	0.004	—	—
Image quality index	0.809 (0.750, 0.867)	<0.001	—	—
Deep capillary plexus				
Female sex	0.252 (−0.038, 0.542)	0.089	—	—
Mean age (yr)	0.013 (0.002, 0.023)	0.011	—	—
BCVA (logMAR)	−10.08 (−14.107, −6.063)	<0.001	−6.170 (−10.175, −2.166)	0.003
IOP (mm Hg)	0.066 (0.009, 0.122)	0.022	—	—
ACD (mm)	−0.621 (−0.872, −0.370)	<0.001	−0.348 (−0.673, −0.023)	0.036
Lens thickness (mm)	0.208 (−0.093, 0.511)	0.176	—	—
AL (mm)	−0.260 (−0.375, −0.146)	<0.001	—	—
GCIPL thickness (μ m)	0.024 (−0.006, 0.054)	0.118	—	—
pRNFL thickness (μ m)	0.006 (−0.007, 0.019)	0.371	—	—
Image quality index	0.198 (0.175, 0.220)	<0.001	—	—

The age, sex, and image quality index were adjusted and analyzed in the multivariate model. Bold values indicate statistical significance.

Ocular Factors of BVT in Each Layer

Factors associated with BVT are listed in Table 4. After adjusting for age, sex, and IQS, superficial FD was significantly correlated with IOP ($\beta = -0.044$; 95% CI, -0.079 to -0.009 ; $P = 0.012$) and AL ($\beta = 0.097$; 95% CI, 0.014 – 0.181 ; $P = 0.022$; $R^2 = 0.10$; RMSE = 2.58). In the multivariate model, IOP ($\beta = -0.004$; 95% CI, -0.009 to -0.005 ; $P = 0.028$) and LT ($\beta = 0.036$; 95% CI, 0.003 – 0.060 ; $P = 0.028$) were associated with FD in the DCP after adjusting for the confounding factors ($R^2 = 0.07$; RMSE = 0.25).

Discussion

This study demonstrated that FD is positively associated with IOP and negatively correlated with axial length in the SCP. In the DCP, a higher FD was correlated with poor BCVA and shallower ACD after adjusting for the age, sex, and image quality index. With regard to BVT, increased superficial BVT was related to lower IOP and longer AL. The higher BVT in the DCP was associated with lower IOP and higher LT. To the best of our knowledge, this is the first study

Table 4. Univariate and Multivariate Regression Analyses for Superficial and Deep Blood Vessel Tortuosity

Characteristics	Univariate Regression		Stepwise Multivariate Regression	
	Coefficient (95% CI)	<i>P</i>	Coefficient (95% CI)	<i>P</i>
Superficial capillary plexus				
Female sex	0.067 (−0.130, 0.266)	0.503	—	—
Mean age (yr)	−0.004 (−0.011, 0.002)	0.219	—	—
BCVA (logMAR)	0.074 (−2.999, 3.147)	0.962	—	—
IOP (mm Hg)	−0.064 (−0.101, −0.026)	0.001	−0.044 (−0.079, −0.009)	0.012
ACD (mm)	0.351 (0.179, 0.524)	0.001	—	—
Lens thickness (mm)	0.887 (0.027, 1.74)	0.053	—	—
AL (mm)	0.273 (0.195, 0.351)	<0.001	0.097 (0.014, 0.181)	0.022
GCIPL thickness (μm)	0.079 (−0.005, 0.002)	0.067	—	—
pRNFL thickness (μm)	0.013 (0.018, 0.091)	0.005	—	—
Image quality index	−0.147 (−0.162, −0.132)	<0.001	—	—
Deep capillary plexus				
Female sex	0.005 (−0.017, 0.028)	0.641	—	—
Mean age (yr)	0.001 (0.0005, 0.002)	0.001	—	—
BCVA (logMAR)	0.499 (0.118, 0.880)	0.010	—	—
IOP (mm Hg)	−0.005 (−0.010, −0.001)	0.010	−0.004 (−0.009, −0.0005)	0.028
ACD (mm)	−0.005 (−0.025, 0.014)	0.594	—	—
Lens thickness (mm)	0.044 (0.021, 0.068)	<0.001	0.036 (0.003, 0.060)	0.028
AL (mm)	−0.001 (−0.010, 0.007)	0.808	—	—
GCIPL thickness (μm)	−0.001 (−0.004, 0.0005)	0.124	—	—
pRNFL thickness (μm)	0.0001 (−0.0009, 0.001)	0.812	—	—
Image quality index	−0.010 (−0.012, −0.009)	<0.001	—	—

The age, sex, and image quality index were adjusted and analyzed in the multivariate model. Bold values indicate statistical significance.

regarding the ocular factors of geometric parameters of macular microvasculature using OCTA in a large healthy population.

The FD in the SCP and BVT in both the SCP and DCP were significantly affected by IOP, which is the most important factor related to glaucoma, although there was limited information on ocular factors on FD and BVT derived from OCTA. Our finding is consistent with previous studies based on retinal photography in glaucoma or IOP. Wu et al.⁹ found that decreased FD was independently associated with ocular hypertension (odds ratio, 1.37; 95% CI, 1.04–1.82). Although primary open-angle glaucoma patients exhibited reduced values of fractal parameters, there was no significant difference in venous tortuosity.²² The studies did not indicate a direct relationship between IOP and vascular complexity; however, Cheng et al.¹⁴ reported that IOP was not an influencing factor on FD in normal-tension glaucoma. In an experiment using pig eyes, the capillary tortuosity decreased significantly as IOP increased,²³ which is potentially the most direct evidence for the effect of IOP on vasculatures.

The above studies were controversial and did not come to a unified conclusion regarding the effect of IOP on retinal vessel complexity. Ours might be the first study showing those results but not demonstrating them in the same way that other authors reporting opposite results have.

Another influencing factor discovered in the present study was AL. Previous studies have investigated the effects of AL on retinal vascular complexity. In a study of 6- to 12-year-old Malay girls, per 1-mm of axial length elongation was associated with a reduction of 0.02 in FD using fundus photography.²⁴ We obtained a similar result in the SCP, but not in the DCP. Using spectral domain OCT (SD-OCT), Liu and colleagues²⁵ found that the FD decreased as a stepwise alteration from mild to extreme myopia ($n = 208$) in both the SCP and DCP, and they were strongly correlated with AL as opposed to refractive error. The potential mechanism of the AL-related alteration of FD may be the continuous stretching of retina as elongation of the eyeball, leading to a gradual decline in FD. This result is consistent with our study of FD in the SCP; however, it is

opposite that for FD in the DCP. This may be because the other images were collected by SD-OCT, whereas our study was based on SS-OCT, which may provide more detailed information in the DCP. Another reason may be the normal AL in our population (23.8 ± 1.16 mm) and shorter than mild myopia (24.92 ± 0.75 mm) in the study by Liu et al.²⁵ Cheung et al.²⁶ used SS-OCTA to investigate the determinants of FD in Hong Kong children ($n = 1059$; 6–8 years of age) and found no correlation between AL and FD.

Another discovery of the present study is that lower FD is correlated with poor BCVA in the DCP. Previous studies by Hisao et al.²⁷ and Shi et al.²⁸ presented similar conclusions in patients with diabetic macular edema and Parkinson's disease in the inferior quadrant, respectively. However, the clinical significance of the relationship between FD in the DCP and visual acuity must be further implemented.

The thickness of the pRNFL and GCIPL mirrors the condition of glaucoma; however, the relationship between vascular complexity and thickness has not been fully investigated. In this study, the average pRNFL thickness was correlated with FD and BVT in the SCP, but in the multivariate model there was no statistical significance. The average GCIPL thickness was not related to either FD or BVT. Tham et al.²⁹ reported that decreased FD was independently associated with a thinner RNFL, and decreased FD and venular tortuosity were independently associated with thinner average GCIPL in non-glaucomatous eyes. However, the study did not conduct segmented analysis based on fundus photos, and our study provided more in-depth information in both the SCP and DCP. A comparison of this study with previous other studies is provided in Supplementary Table S1. In this study, the main values of all geometric parameters exhibited a slight difference within the age range of around 40 to 70 years, which implied a limited change of these parameters with a period of 30 years. This finding hinted that the ageing effect will not become an important factor for these parameters. In contrast, the ocular factors evaluated in this study, such as IOP and AL, should be considered in further evaluations of glaucoma or myopia.

The advantages of the current study are as follows: First, this is the first study of quantitative macular microvascular complexity using SS-OCTA in a normal population. Second, this study had a relatively large sample size (2189 subjects, 2189 eyes) with a single ethnicity; ethnic heterogeneity would have increased the chance of confounding the findings. Third, novel SS-OCTA was used, which is better able to visualize microvasculature in different segments. The faster scanning speed of SS-OCTA allows a relatively large

capture area (6×6 mm) that contains more information than obtained by previous studies. Fourth, the ocular factors regarding vascular complexity were systematically studied, thus offering reference values for future research.

The present study has some limitations. First, this study did not include any ocular disorders, and conclusions cannot be extrapolated to diseased eyes. Future studies with similar analyses could be performed for patients with several ocular diseases. Second, this was a cross-sectional study that utilized hospital-based data, thus limiting the ability to infer causality and determine retinal vasculature alterations. A longitudinal study is needed to demonstrate the causal relationships among FD, BVT, and their associated factors. Third, the cohort included only Chinese subjects, and the images were obtained using a specific OCTA device, thus limiting the application of our findings to other ethnicities, and it is not clear that similar results would be obtained by other OCTA devices. Finally, the goodness of the regression model was perfect, indicating that other studies should further explore the ocular factors related to FD and BVT.

To conclude, this study has reported macular FD and BVT in a healthy Chinese population and explored their ocular factors. The IOP, AL, BCVA, ACD, and LT were independent factors for FD and BVT in the various layers, and future studies should consider these factors.

Acknowledgments

The authors thank all of the technicians and clinical research collaborators of the clinical research center at ZOC.

Supported by the High-Level Hospital Construction Project, Zhongshan Ophthalmic Center, Sun Yat-sen University (303020104); the National Natural Science Foundation of China (82070955); and the Science and Technology Program of Guangzhou, China.

Disclosure: **Y. Song**, None; **W. Cheng**, None; **F. Li**, None; **F. Lin**, None; **P. Wang**, None; **X. Gao**, None; **Y. Peng**, None; **Y. Liu**, None; **H. Zhang**, None; **S. Chen**, None; **Y. Fan**, None; **R. Zhang**, None; **W. Wang**, None; **X. Zhang**, None

* YS and WC contributed equally to this work.

References

- Steinmetz JD, Bourne RRA, Briant PS, et al. Causes of blindness and vision impairment in 2020 and trends over 30 years, and prevalence of avoidable blindness in relation to VISION 2020: the Right to Sight: an analysis for the Global Burden of Disease Study. *Lancet Glob Health*. 2021;9(2):e144–e160.
- Taylor HR. Global blindness: the progress we are making and still need to make. *Asia Pac J Ophthalmol (Phila)*. 2019;8(6):424–428.
- Yarmohammadi A, Zangwill LM, Diniz-Filho A, et al. Relationship between optical coherence tomography angiography vessel density and severity of visual field loss in glaucoma. *Ophthalmology*. 2016;123(12):2498–2508.
- Moghimi S, Hou H, Rao H, Weinreb RN. Optical coherence tomography angiography and glaucoma: a brief review. *Asia Pac J Ophthalmol (Phila)*. 2019.
- Shin JW, Lee J, Kwon J, et al. Relationship between macular vessel density and central visual field sensitivity at different glaucoma stages. *Br J Ophthalmol*. 2019;103(12):1827–1833.
- Yarmohammadi A, Zangwill LM, Diniz-Filho A, et al. Peripapillary and macular vessel density in patients with glaucoma and single-hemifield visual field defect. *Ophthalmology*. 2017;124(5):709–719.
- Lin F, Li F, Gao K, et al. Longitudinal changes in macular optical coherence tomography angiography metrics in primary open-angle glaucoma with high myopia: a prospective study. *Invest Ophthalmol Vis Sci*. 2021;62(1):30.
- Li F, Lin F, Gao K, et al. Association of foveal avascular zone area with structural and functional progression in glaucoma patients [published online ahead of print April 7, 2021]. *Br J Ophthalmol*, <https://doi.org/10.1136/bjophthalmol-2020-318065>.
- Wu R, Cheung CY, Saw SM, Mitchell P, Aung T, Wong TY. Retinal vascular geometry and glaucoma: the Singapore Malay Eye Study. *Ophthalmology*. 2013;120(1):77–83.
- Chan K, Tang F, Tham C, Young AL, Cheung CY. Retinal vasculature in glaucoma: a review. *BMJ Open Ophthalmol*. 2017;1(1):e000032.
- Lin T, Wang YM, Ho K, et al. Global assessment of arteriolar, venular and capillary changes in normal tension glaucoma. *Sci Rep*. 2020;10(1):19222.
- Rudnicka AR, Owen CG, Welikala RA, et al. Retinal vasculometry associations with glaucoma: findings from the European Prospective Investigation of Cancer-Norfolk Eye Study. *Am J Ophthalmol*. 2020;220:140–151.
- Hou H, Moghimi S, Proudfoot JA, et al. Ganglion cell complex thickness and macular vessel density loss in primary open-angle glaucoma. *Ophthalmology*. 2020;127(8):1043–1052.
- Cheng K, Tan BL, Brown L, et al. Macular vessel density, branching complexity and foveal avascular zone size in normal tension glaucoma. *Sci Rep*. 2021;11(1):1056.
- Cheng W, Song Y, Lin F, et al. Assessment of artifacts in swept-source optical coherence tomography angiography for glaucomatous and normal eyes. *Transl Vis Sci Technol*. 2022;11(1):23.
- Kamalipour A, Moghimi S, Hou H, et al. OCT angiography artifacts in glaucoma. *Ophthalmology*. 2021;128(10):1426–1437.
- Wen C, Pei C, Xu X, Lei J. Influence of axial length on parafoveal and peripapillary metrics from swept source optical coherence tomography angiography. *Curr Eye Res*. 2019;44(9):980–986.
- Bennett AG, Rudnicka AR, Edgar DF. Improvements on Littmann's method of determining the size of retinal features by fundus photography. *Graefes Arch Clin Exp Ophthalmol*. 1994;32(6):361–367.
- You QS, Tan O, Pi S, et al. Effect of algorithms and covariates in glaucoma diagnosis with optical coherence tomography angiography [published online ahead of print June 28, 2021]. *Br J Ophthalmol*, <https://doi.org/10.1136/bjophthalmol-2020-318677>.
- Fan W, Nittala MG, Fleming A, et al. Relationship between retinal fractal dimension and non-perfusion in diabetic retinopathy on ultrawide-field fluorescein angiography. *Am J Ophthalmol*. 2020;209:99–106.
- Falconer K. *Fractal Geometry: Mathematical Foundations and Applications*. 2nd ed. Chichester: John Wiley & Sons; 2003:90–98.
- Chiquet C, Gavard O, Arnould L, et al. Retinal vessel phenotype in patients with primary open-angle glaucoma. *Acta Ophthalmol*. 2020;98(1):e88–e93.
- Brazile BL, Yang B, Waxman S, et al. Lamina cribrosa capillaries straighten as intraocular pressure increases. *Invest Ophthalmol Vis Sci*. 2020;61(12):2.
- Tai EL, Li LJ, Wan-Hazabbah WH, Wong T-Y, Shatriah I. Effect of axial eye length on retinal vessel parameters in 6 to 12-year-old Malay girls. *PLoS One*. 2017;12(1):e0170014.
- Liu M, Wang P, Hu X, Zhu C, Yuan Y, Ke B. Myopia-related stepwise and quadrant retinal

- microvascular alteration and its correlation with axial length. *Eye (Lond)*. 2021;35(8):2196–2205
26. Cheung CY, Li J, Yuan N, et al. Quantitative retinal microvasculature in children using swept-source optical coherence tomography: the Hong Kong Children Eye Study [published online ahead of print June 28, 2018]. *Br J Ophthalmol*, <https://doi.org/10.1136/bjophthalmol-2018-312413>.
 27. Hsiao CC, Yang CM, Yang CH, Ho T-C, Lai T-T, Hsieh Y-T. Correlations between visual acuity and macular microvasculature quantified with optical coherence tomography angiography in diabetic macular oedema. *Eye (Lond)*. 2020;34(3):544–552.
 28. Shi C, Chen Y, Kwapong WR, et al. Characterization by fractal dimension analysis of the retinal capillary network in Parkinson disease. *Retina*. 2020;40(8):1483–1491.
 29. Tham YC, Cheng CY, Zheng Y, Aung T, Wong TY, Cheung CY. Relationship between retinal vascular geometry with retinal nerve fiber layer and ganglion cell-inner plexiform layer in nonglaucomatous eyes. *Invest Ophthalmol Vis Sci*. 2013;54(12):7309–7316.